

V_{S30} Characterization of Texas, Oklahoma, and Kansas Using the P-Wave Seismogram Method

Georgios Zalachoris,^{a)} Ellen M. Rathje,^{b)} M.EERI, and Jeffrey G. Paine^{c)}

The P-wave seismogram method is used to develop estimates of the time averaged shear wave velocity of the upper 30 m (V_{S30}) at 251 seismic stations in Texas, Oklahoma, and Kansas. Geologic conditions at the sites are documented using large-scale geologic maps. The V_{S30} values from the P-wave seismogram method agree well with the limited in situ measurements across the study area and correlate well with the mapped geologic units. Compared with the V_{S30} proxy values assigned to the stations by the Next Generation Attenuation–East (NGA-East) project, the P-wave seismogram method generally produces larger V_{S30} estimates. These differences are likely due to the fact that very few V_S measurements in Texas, Oklahoma, and Kansas were available for use in the development of the NGA-East proxies. Analysis of the P-wave seismogram V_{S30} values indicates that, in this geographic area, incorporating rock type along with geologic age better distinguishes the average V_{S30} of these materials than geologic age alone. [DOI: 10.1193/102416EQS179M]

INTRODUCTION

Seismicity rates in some areas of central and eastern North America (CENA), such as north Texas/Oklahoma/south Kansas, have increased by more than an order of magnitude over the last several years (Petersen et al. 2016). This enhanced seismicity has increased the interest in ground motion prediction equations (GMPEs) for these areas, and has highlighted the need for more detailed site characterization at ground motion recording stations.

The time-averaged shear wave velocity of the upper 30 m of the crust (V_{S30}) has become the standard measure for the subsurface geotechnical/geologic conditions at a site and the evaluation of ground motion amplification in GMPEs (e.g., Abrahamson et al. 2014, Boore et al. 2014). Due to the lack of existing in-situ measurements of shear wave velocity profiles at recording stations in CENA (only 6% of the stations included in NGA-East database have measured V_{S30} values, Goulet et al. 2014), V_{S30} proxy methods have been used to estimate V_{S30} values at most of the recording sites used in the development of GMPEs for CENA. Proxy methods relate V_{S30} to parameters such as surface geology, topographic slope, or

^{a)} Visiting Scholar – Post Doctoral Fellow, Dept. of Civil, Architectural, and Environmental Engineering, Univ. of Texas, Austin, TX 78712

^{b)} Warren S. Bellows Professor, Dept. of Civil, Architectural, and Environmental Engineering, Univ. of Texas, Austin, TX 78712

^{c)} Senior Research Scientist, Bureau of Economic Geology, Jackson School of Geosciences, Univ. of Texas, Austin, TX 78713

terrain. These proxy methods have been developed predominantly for active tectonic regions, such as [Wills and Clahan \(2006\)](#) for geology, [Wald and Allen \(2007\)](#) for topographic slope, and [Yong et al. \(2012\)](#) for terrain. For CENA, [Kottke et al. \(2012\)](#) developed geology-based V_{S30} proxy relationships by dividing the geologic conditions into 19 categories based on factors such as glaciation, the presence of residual soils, geologic age and depositional environment. [Parker et al. \(2017\)](#) revised the work of [Kottke et al. \(2012\)](#) to develop a hybrid geology-slope proxy method for CENA based on statistical analysis of 2,754 sites with measured V_{S30} values. The sites were grouped by attributes including geologic age, lithology, glaciation history and location relative to known basins, and the relationship between V_{S30} and 30 arc-second slope gradients was also taken into account for some groups. This work was done as part of the Next Generation Attenuation - East (NGA-East) project (<http://peer.berkeley.edu/ngaeast/>).

An alternative to the proxy methods is the P-wave seismogram method ([Kim et al. 2016](#), [Ni et al. 2014](#), [Hosseini et al. 2016](#)), which estimates V_{S30} from the recorded ground motions at a site using the fundamentals of wave propagation. [Kim et al. \(2016\)](#) showed that the P-wave seismogram method predicts V_{S30} with less bias and less variability than the various proxy methods. As a result, we chose to apply the P-wave seismogram method to estimate V_{S30} for seismic stations located in the central midcontinent states of Texas, Oklahoma, and Kansas. These V_{S30} estimates are compared with the mapped geology from large-scale geologic maps and with those predicted by the [Parker et al. \(2017\)](#) hybrid geology-slope proxy method for CENA. An electronic supplement is provided that compiles the recording stations for which the P-wave seismogram method was applied, the P-wave seismogram results, and geologic descriptions for the seismic stations.

P-WAVE SEISMOGRAM METHOD

The P-wave seismogram method is based on the fact that propagating seismic waves tend to be refracted to a more vertical position as they travel through softer material towards the ground surface. As a result, the vertical component of the P-wave amplitude tends to be larger than the radial component for softer sites. The analytical expressions in [Aki and Richards \(2002\)](#) for the radial and vertical displacement at the free surface from a single P-wave with an incident angle i (Figure 1a), can be used to derive an expression for the ratio of the radial to vertical particle velocity:

$$\frac{\dot{U}_R}{\dot{U}_Z} = \frac{2V_S p \cos j}{1 - 2p^2 V_S^2} \quad (1)$$

where \dot{U}_R is the radial particle velocity, \dot{U}_Z is the vertical particle velocity, V_S is the shear wave velocity of the medium, j is the angle of the reflected SV wave, and p is the ray parameter. Solving for V_S , we obtain:

$$V_S = \frac{\cos j \pm \sqrt{\cos^2 j + 2 \left(\frac{\dot{U}_R}{\dot{U}_Z} \right)^2}}{-2p \left(\frac{\dot{U}_R}{\dot{U}_Z} \right)} \quad (2)$$

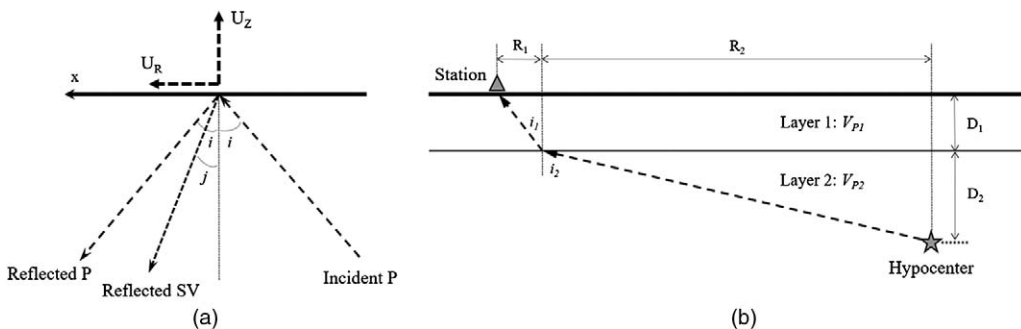


Figure 1. Schematic of: (a) reflection of incident P-wave at the free surface, (b) simplified two-layer system used for computations in P-wave Seismogram method. U_R and U_Z are the radial and vertical particle displacements, respectively.

The ray parameter, p , and the angle j are related and can be expressed as:

$$p = \frac{\sin i}{V_P} = \frac{\sin j}{V_S} \tag{3}$$

$$j = \sin^{-1}(pV_S). \tag{4}$$

The particle velocities \dot{U}_R and \dot{U}_Z can be retrieved from recorded velocity time series or integration of recorded acceleration time series with the horizontal components rotated to the direction of the azimuth between the earthquake epicenter and the seismic station. Kim et al. (2016) used the initial portions of the time series to select the first peak value of (\dot{U}_Z) and then the corresponding value of (\dot{U}_R) at the same moment in time.

Kim et al. (2016) estimated the ray parameter, p , by assuming a simplified two-layer crustal velocity model, as shown in Figure 1b:

$$p = \frac{\sin\left(\tan^{-1}\left(\frac{R_1}{D_1}\right)\right)}{V_{P_1}} = \frac{\sin\left(\tan^{-1}\left(\frac{R_2}{D_2}\right)\right)}{V_{P_2}} \tag{5}$$

where R_1 and R_2 are the horizontal distances travelled in the upper and lower layers, respectively, D_1 is the thickness of the upper layer, D_2 is the hypocentral depth minus D_1 , V_{P_1} and V_{P_2} are the P-wave velocities of the upper and lower layers, respectively, and R is the epicentral distance and equal to $R_1 + R_2$ (Figure 1b). V_{P_1} , V_{P_2} , and D_1 are obtained based on an assumed crustal velocity model. To apply the P-wave seismogram proxy method, Kim et al. (2016) utilized the crustal velocity models developed by the Electric Power Research Institute (EPRI) for CENA (EPRI 1993).

The P-wave seismogram method is applied as follows: (1) assume a value of angle j ; (2) estimate the ray parameter, p , using Equation 5; (3) compute V_S using Equation 2; (4) compute a new value of angle j using Equation 4; and (5) repeat steps 3 and 4 until two consecutively computed values of angle j fall within a predetermined level of tolerance.

The estimated V_S value is representative of the time-averaged shear wave velocity of the upper z meters (V_{SZ}). Kim et al. (2016) assumed that the depth z is estimated as the product of the pulse duration of the source time function and the estimated shear wave velocity ($z = \tau_p \cdot V_{SZ}$), an expression which is equivalent to the wavelength of the S-wave. The authors recommended a value of τ_p equal to 0.1 s which they considered appropriate for small magnitude earthquakes ($M = 3-4$). The final step of the P-wave seismogram method is the conversion of V_{SZ} to V_{S30} . Kim et al. (2016) used 821 published measured shear wave velocity profiles in CENA to develop regression relationships between V_{SZ} and V_{S30} . The regression was performed separately for glaciated and non-glaciated regions.

APPLICATION OF P-WAVE SEISMOGRAM METHOD

To obtain a substantial number of earthquake ground motions to be used for the development of V_{S30} estimates at seismic station locations in Texas, Oklahoma, and Kansas, a catalog of earthquake events with epicenters located in the region was created using the comprehensive database accessed via the website of the Incorporated Research Institutions for Seismology, IRIS (<https://www.iris.edu/hq/>). Earthquake events occurring after January 2005 within a specified area (Figure 2a), with magnitudes greater than 3.0, were selected. The locations and magnitudes of the selected earthquakes are illustrated in Figure 2a. More than 400 seismic recording stations were operational in Texas, Oklahoma, and Kansas at some time between 2005 and 2015 (Figure 2b). A substantial effort was made to apply the P-wave seismogram method to all the seismic stations illustrated in Figure 2b. Due to the large epicentral distances and the associated weak signals and/or the increased noise levels at many of

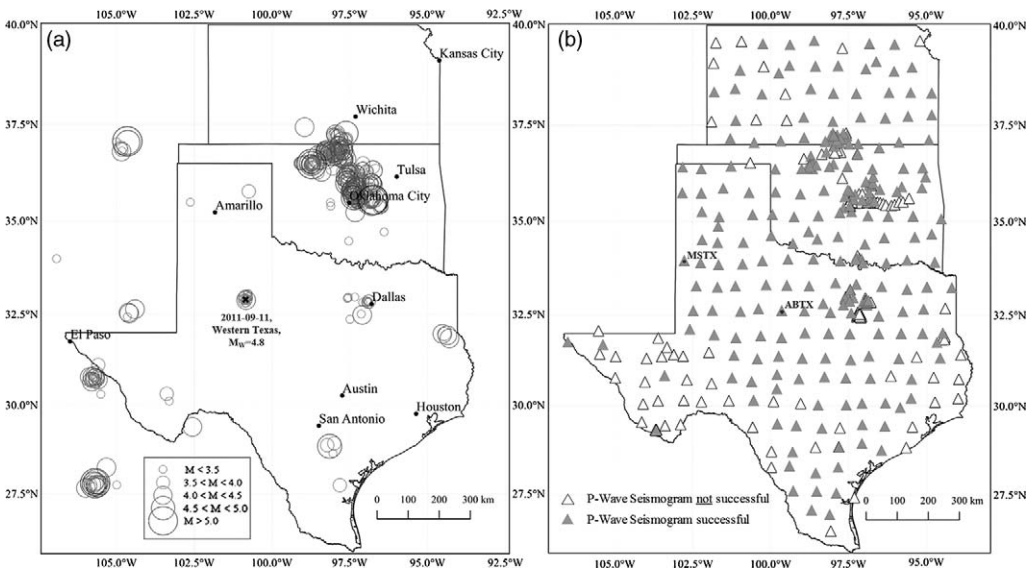


Figure 2. Locations of (a) selected earthquake events, and (b) seismic recordings stations in Texas, Oklahoma and Kansas.

the seismic stations, the P-wave seismogram was successfully implemented for only 251 of the available seismic stations.

Ground motion data recorded at the 251 stations were retrieved using tools available on the website of IRIS (i.e., Standing Order for Data, or SOD, software, <https://ds.iris.edu/ds/nodes/dmc/software/downloads/sod/>). All collected time series were processed in a uniform manner. The downloaded recordings were instrument corrected (i.e., instrument response was removed), the mean was removed and linear detrending was performed. The records were examined for obvious irregularities (i.e., clipping, distortion, apparent high noise) on an individual basis. Any records with signal-to-noise ratio (SNR) persistently less than 3 within the bandwidth of the recording instrument were rejected. Finally, three-component velocity time series were obtained for each record. A total of 2,871 processed recordings were used to estimate V_{S30} at the 251 seismic stations.

Once the appropriate velocity time series were identified, the P-wave seismogram method was applied, as described above. For the purposes of this study, we utilized the crustal velocity models developed by EPRI (1993). For Texas, Oklahoma, and Kansas, the crustal velocity structures associated with the Gulf Coast Plain, the Southern Great Plains, and the Central Plains were used. Table 1 presents these crustal velocity models. To test the sensitivity of the results to the assumed crustal velocity models, separate V_{SZ} estimates were obtained using an alternative set of crustal velocity models from the NGA-East project (Dreiling et al. 2014, Table 1). Using these velocity models, the average effect on the estimated V_{S30} values is on the order of 2% to 7%, which is considered minimal.

Table 1. Crustal velocity models used in P-wave Seismogram method

EPRI (1993) Crustal Velocity Models								
Gulf Coast Plain			Southern Great Plains			Central Plains		
Layer	Thickness (km)	V_p (km/s)	Layer	Thickness (km)	V_p (km/s)	Layer	Thickness (km)	V_p (km/s)
1	7	4	1	2	5	1	3	4.5
2	8	5.3	2	14	6.1	2	22	6.2
3	15	6.5	3	15	6.7	3	15	6.7
4	–	8.2	4	14	7.2	4	–	7.9
			5	–	8.2			

NGA-E (Dreiling et al. 2014) Crustal Velocity Models					
Gulf Coast/Mississippi Embayment			Central North America		
Layer	Thickness (km)	V_p (km/s)	Layer	Thickness (km)	V_p (km/s)
1	4	5.9	1	12	6.1
2	12.5	6.2	2	8	6.5
3	13.5	6.6	3	14	6.7
4	11	7.3	4	6	6.8
5	–	8	5	–	8.1

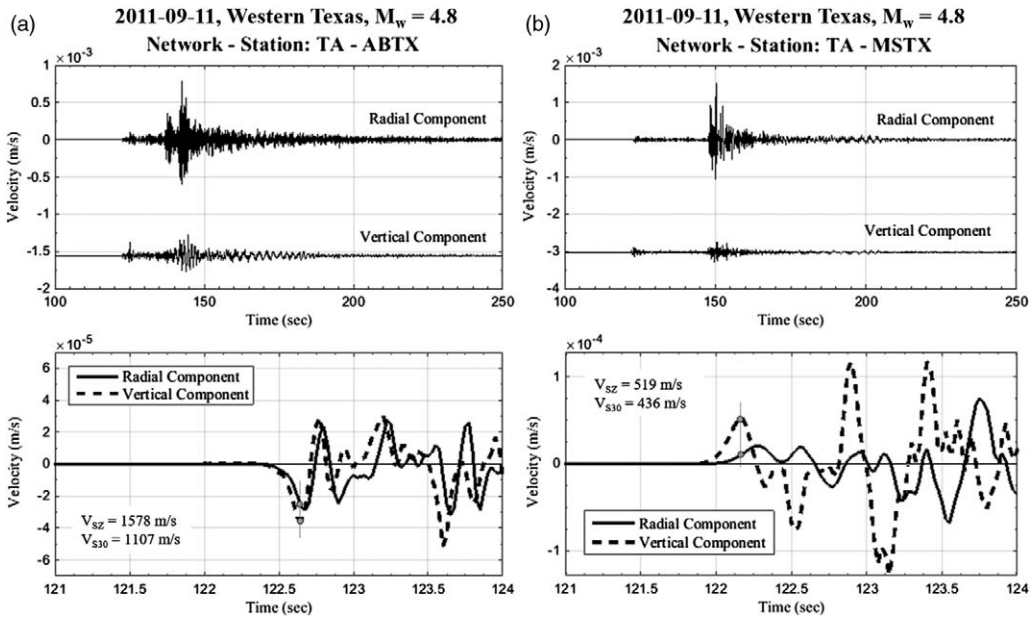


Figure 3. Example application of P-wave Seismogram method for (a) ABTX seismic station, and (b) MSTX seismic station.

Figure 3 illustrates two example applications of the P-wave Seismogram method for the ABTX and MSTX seismic stations (locations of these stations are shown in Figure 2), both of which belong to the Transportable Array network (TA). The ground motions depicted in Figure 3 were recorded during the 11 September 2011, $M_w = 4.8$ earthquake event in western Texas (Figure 2a). For seismic station ABTX (Figure 3a) the radial \dot{U}_R and vertical \dot{U}_Z components of the velocity time series have similar amplitudes, while for seismic station MSTX (Figure 3b) \dot{U}_R and \dot{U}_Z are substantially different. Based on the theoretical concept of the P-wave seismogram method, it can be concluded that ABTX is a stiffer site (i.e., larger incident angle i in Figure 1a), while MSTX is a softer site (i.e., smaller incident angle i in Figure 1a). The computed V_{SZ} values for ABTX and MSTX, are 1,578 m/s and 519 m/s, respectively. These V_{SZ} values are representative of the upper $0.1 \times 1,578 \approx 158$ m and $0.1 \times 519 \approx 52$ m of the velocity profiles at the ABTX and MSTX sites, respectively. Finally, using the regression parameters developed by Kim et al. (2016) for CENA, the V_{SZ} values are converted to V_{S30} . The V_{S30} estimate for ABTX is 1,107 m/s, while for MSTX the estimated V_{S30} value is 436 m/s.

The procedure described above was applied to all records considered. Consequently, V_{SZ} values were estimated for 251 seismic stations (Figure 2b) based on 2,871 individual records. Figure 4 shows the box plots of the computed V_{SZ} values for a subset of the seismic stations considered in this study. These stations were selected to demonstrate the range of results obtained at the 251 sites. The median V_{SZ} values for the stations in Figure 4 range from less than 100 m/s for GS.OK035 to more than 2,500 m/s for US.WMOK, and the variability

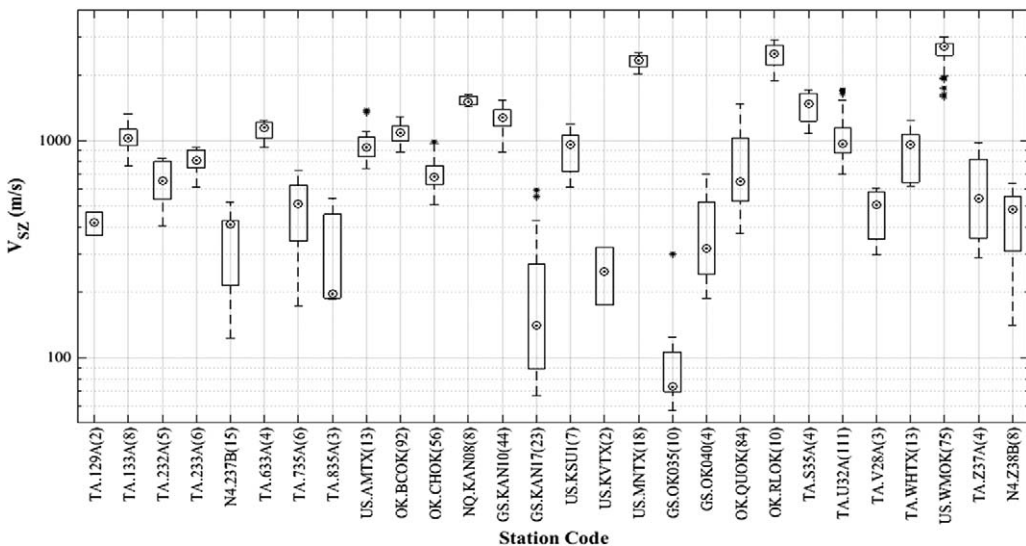


Figure 4. Computed V_{SZ} values for a subset of seismic stations considered in this study. Number in parentheses next to the station code refers to the number of V_{SZ} estimates. Minimum and maximum values of V_{SZ} are depicted in single line bars, the 25th and 75th percentiles are depicted within the box plots, the median value is shown by single points, while outliers are shown as asterisks.

in the V_{SZ} values vary from site to site. Some stations have a substantial number of V_{SZ} estimates (i.e., 111 estimates for TA.U32A), while others have only a couple of V_{SZ} estimates. Overall, 36% of the seismic stations analyzed have at least 5 V_{SZ} estimates, while 26% have only one V_{SZ} estimate.

Figure 5 summarizes the number of P-wave seismogram V_{S30} estimates and the $\sigma_{ln V}$ of these V_{S30} estimates as a function of the median estimated V_{S30} for each seismic station. Figure 5a shows that the stiffer sites tend to have more seismograms for which the P-wave seismogram method successfully estimated a V_{S30} . This effect is due to the fact stiffer sites tend to be less noisy and thus it is easier to identify the P-wave arrival. The $\sigma_{ln V}$ values in Figure 5b vary considerably from site to site because the variability in the V_{S30} estimates at a given site is influenced by the number of recordings, the noise in the records, and various assumptions. Generally, $\sigma_{ln V}$ is smaller at the larger V_{S30} sites, with an average $\sigma_{ln V}$ of 0.12 at sites with V_{S30} greater than 1,000 m/s and an average $\sigma_{ln V}$ of 0.24 at sites with V_{S30} smaller than 500 m/s.

V_{S30} VALUES ACROSS TEXAS, OKLAHOMA, AND KANSAS

Maps of the median V_{SZ} and V_{S30} estimates from the P-wave Seismogram method for the 251 seismic stations in Texas, Oklahoma, and Kansas are shown in Figure 6. The discrete values are shown in terms of 5 bins: $V_S \leq 200$ m/s, 200 m/s $< V_S \leq 400$ m/s, 400 m/s $< V_S \leq 760$ m/s, 760 m/s $< V_S \leq 1,500$ m/s, and $V_S > 1,500$ m/s. The

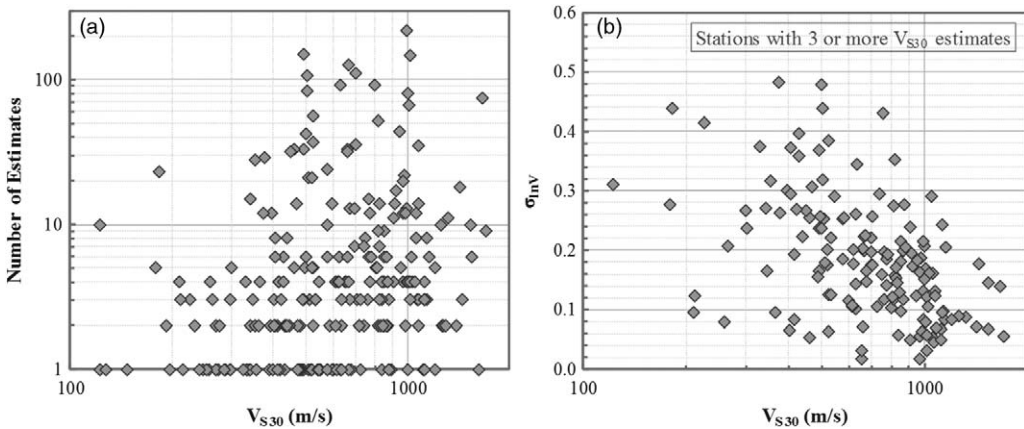


Figure 5. (a) Number of V_{S30} estimates for each station as a function of the estimated V_{S30} and (b) standard deviation of the natural logarithm of V_{S30} ($\sigma_{\ln V}$) for each station as a function of the estimated V_{S30} .

smallest V_{S30} value in the study area was from 10 recordings at GS.OK035 in western Oklahoma ($V_{S30} = 123$ m/s), while the largest V_{S30} was computed from nine recordings at TA.V37A in southeastern Kansas ($V_{S30} = 1,706$ m/s). A continuous map of interpolated V_{S30} was developed (Figure 6c) using the V_{S30} estimates and inverse distance weighting (IDW) interpolation based on 3 neighboring points. To demonstrate the relationship between the P-wave seismogram results and the geologic features across the study area, the digital state-wide geologic maps compiled by the United States Geological Survey (USGS) Division of Mineral Resources (DMR) (<http://mrddata.usgs.gov/geology/state/>) for Texas, Oklahoma, and Kansas are shown in Figure 6d. It is important to note that the interpolated V_{S30} values shown in Figure 6c do not capture local variations in geology and subsurface conditions, because the spacing of the seismic stations at which V_{S30} was estimated is relatively large (i.e., ~ 70 km across much of the study area). This issue is even more relevant in the Basin and Range region in western Texas, where the spacing between V_{S30} estimates is 200 to 300 km. Nonetheless, the map in Figure 6c still provides a useful visualization of the V_{S30} distribution across the study area.

Figure 6 shows that the computed V_{S30} values are smaller (i.e., < 400 m/s) along the Gulf Coast and within the Dallas-Fort Worth (DFW) area, and near the Panhandle region of western Oklahoma. The Gulf Coast is characterized by a broad plain of Quaternary and Tertiary unconsolidated material (alluvium, terrace, clay, silt, sand deposits; Figure 6d) and the stations in the DFW area are located mostly on Holocene alluvium deposited by the Trinity River. These geologic descriptions are consistent with the estimated V_{S30} values of less than 400 m/s.

The V_{S30} values in Figure 6 are higher (i.e., > 760 m/s) within the Llano Uplift and North-Central Plains in Texas, the Wichita and Arbuckle Mountains in southern Oklahoma,

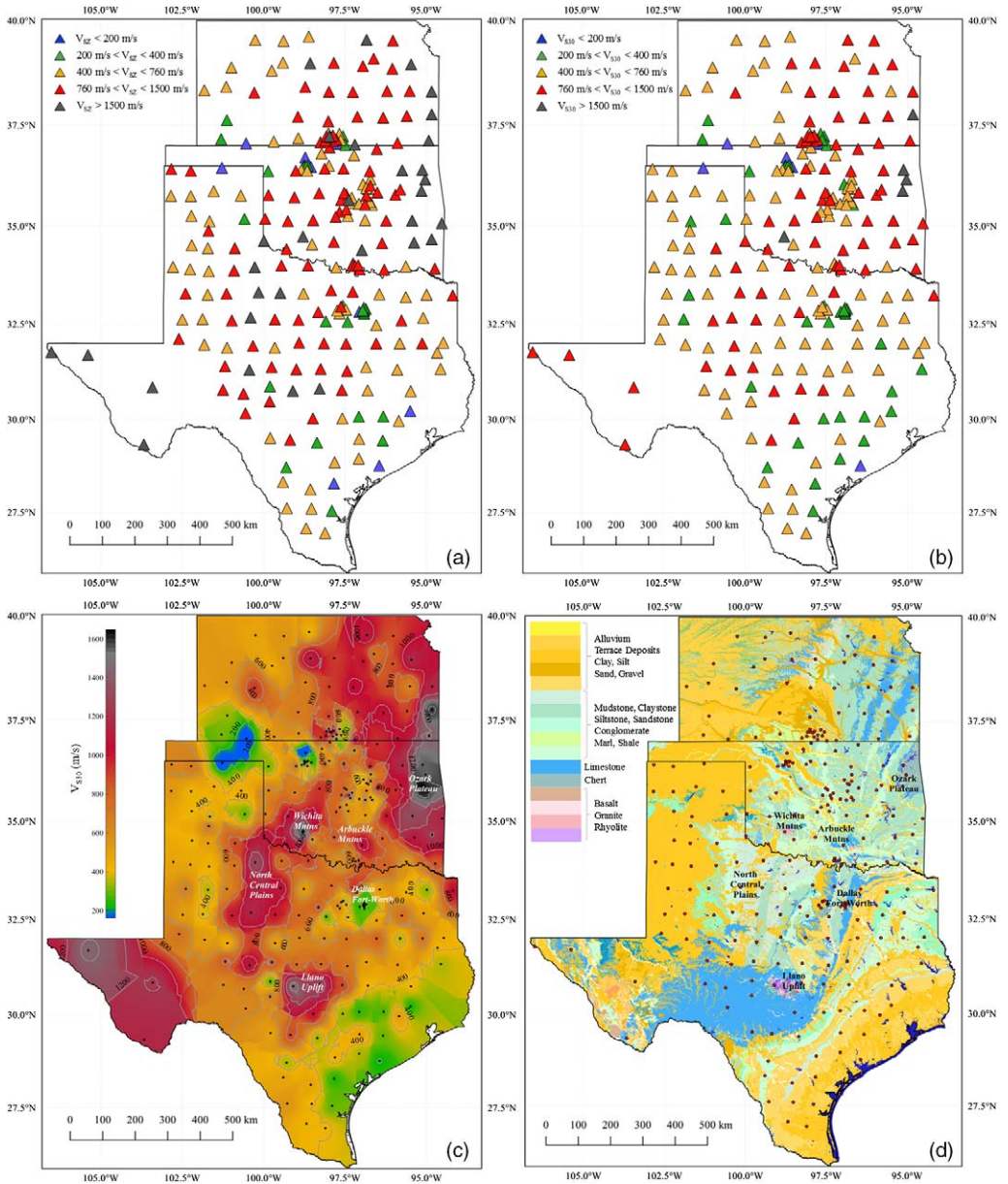


Figure 6. Distribution of V_{S30} across Texas, Oklahoma, and Kansas: (a) color-coded stations based on median V_{SZ} estimates, (b) color-coded stations based on median V_{S30} estimates, (c) interpolated map based on median V_{S30} estimates, and (d) USGS DMR state-wide geologic maps. Points in (c) and (d) represent V_{S30} estimate locations. (Figure is in color online.)

and the Ozark Plateau in eastern Oklahoma and southeastern Kansas. These areas are characterized by Precambrian and Paleozoic igneous and metamorphic rocks (Llano Uplift in Central Texas and Wichita and Arbuckle mountains in south-central Oklahoma), Paleozoic chert and limestone formations (Ozark Plateau), Paleozoic shales, siltstones, and sandstones (North Central Plains), and Paleozoic shale and limestone units (eastern Kansas).

The Permian Basin of Texas, the Panhandle regions of Texas and Oklahoma, and the west Kansas region are part of the Great Plains and consist predominantly of Quaternary wind-blown sands and silts (e.g., Blackwater Draw Formation) with some alluvium (Figure 6d). Figure 6 shows that the V_{S30} values in this region areas are consistently larger than 400 m/s, with some locations larger than 760 m/s. These values of V_{S30} are larger than one would generally expect for Quaternary deposits. These large values of V_{S30} may be caused by the fact that the thickness of the surficial windblown and alluvial deposits in some places is much less than 30 m (as indicated by the geologic descriptions in the geologic maps), and in these locations the P-wave seismogram V_{S30} estimates would reflect the characteristics of both the relatively thin surficial sediments and the underlying stiffer formations.

The P-wave seismogram V_{S30} estimates can be compared with a limited number of V_{S30} values from in-situ measurements obtained in the region, as reported by the NGA-East project (Parker et al. 2017). From a total of 2,754 in-situ V_S measurement locations in the NGA-East database, 78 lie within Texas, Oklahoma, and Kansas. Sixty-eight of these measurements were performed along the Texas Gulf Coast, with most of the rest performed in Oklahoma. Only one of these measurements is co-located with a P-wave seismogram estimate of V_{S30} from this study (US.WMOK station in the Wichita Mountains of Oklahoma). The in situ shear wave velocity measurement at the US.WMOK seismic station indicates a value of $V_{S30} = 1,859$ m/s, while the P-wave seismogram method estimated a V_{S30} value of 1,663 m/s. This is considered excellent agreement with only about 10% difference. Additional in-situ shear wave velocity measurements have been collected at 15 seismic stations in the Dallas-Fort Worth area (Zalachoris et al. 2017). The V_{S30} values from in-situ measurements are plotted against the values estimated by the P-wave seismogram method in Figure 7. The agreement is favorable with data scattered about a 1:1 line. A slight negative bias is indicated (i.e., the P-wave seismogram values are about 20% smaller than the values from the in-situ measurements, on average), but this bias generally is within the uncertainty of the V_{S30} measurement.

The generally favorable comparisons with in situ measurements provide some confidence in the estimates of V_{S30} from the P-wave seismogram method. Nonetheless, a further assessment of the performance and variability of the P-wave seismogram method using measured V_S profiles in different areas and geologic units, particularly at locations of seismic stations within Texas, is necessary. Additionally, it is important to note that obtaining V_{S30} from in-situ shear wave velocity measurements is always preferred over any other method.

COMPARISON WITH NGA-EAST V_{S30} ESTIMATES

As mentioned earlier, Parker et al. (2017) developed a hybrid slope-geology based proxy method for the CENA and this method was used to assign V_{S30} values to 1,378 seismic stations in CENA (Goulet et al. 2014). One-hundred eighty-two of these stations correspond with stations analyzed by the P-wave seismogram method in this study.

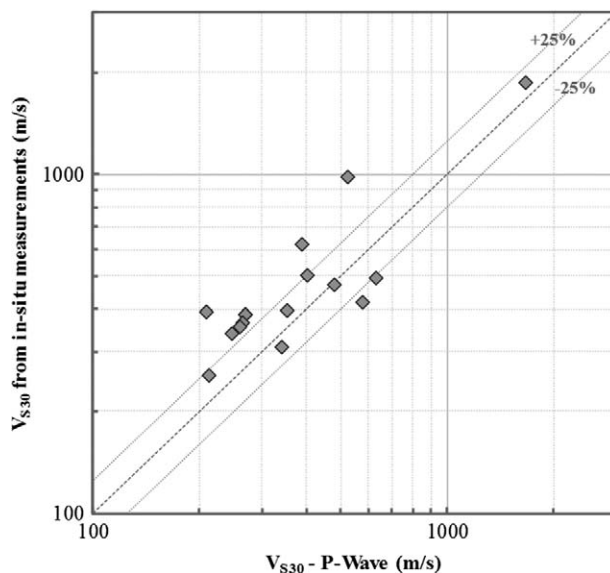


Figure 7. Comparison of estimated P-wave seismogram V_{S30} values with V_{S30} values obtained from in-situ measurements at co-located seismic stations.

Figure 8 compares the P-wave seismogram V_{S30} estimates of the present study with those from Parker et al. (2017) for NGA-East for the stations common in the data sets. For 37% of the seismic stations the V_{S30} estimates from the hybrid slope-geology proxy method and the P-wave seismogram method are within $\pm 25\%$ of each other. The P-wave seismogram method estimates are more than 25% smaller than the NGA-East estimates for 15% of the stations (these are predominantly Mesozoic sites), and they are more than 25% larger than the NGA-East estimates for 48% of the stations (these are predominantly Quaternary, Tertiary, and Paleozoic sites).

For stations located on Paleozoic units (i.e., Llano Uplift, North-Central Plains, Wichita and Arbuckle mountains, Ozark Plateau) the NGA-East proxy assigns a V_{S30} of 684 m/s to each site, while the P-wave seismogram method provides a range of estimates that extend to much larger values. For example, the US.WMOK station with an in situ measured V_{S30} of 1,859 m/s and P-wave seismogram estimate of 1,663 m/s falls into this category. These differences with the NGA-East proxy values is possibly due to the Paleozoic V_S measurements in the NGA-East database representing weathered Paleozoic sites that are different than those in the study area of Texas, Oklahoma, and Kansas. Parker et al. (2017) recognized the limitations of their hybrid slope-geology proxy for Paleozoic formations based on the large variability in the measured V_{S30} values for this unit.

The other condition for which the P-wave seismogram estimates of V_{S30} are larger is for the stations located on Quaternary and Tertiary units. Here the NGA-East proxy method assigns V_{S30} between 200 m/s and 400 m/s, and the P-wave seismogram method estimates larger V_{S30} values possibly due to the relatively small thickness of the younger sediments underlain by stiffer geologic units in parts of the study area. As noted earlier, this observation

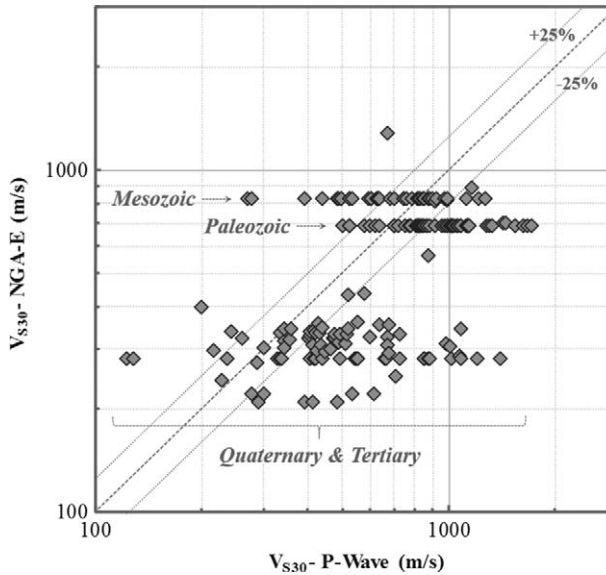


Figure 8. Comparison of V_{S30} estimates from NGA-East (Parker et al. 2017) and from the P-wave Seismogram method in this study.

is particularly relevant for the Quaternary and Tertiary sand deposits in the Permian Basin and Panhandle regions in Texas (e.g., Blackwater Draw Formation and windblown sands), and the Quaternary eolian silts and alluvium deposits in western Kansas.

GROUPING OF V_{S30} ESTIMATES BASED ON GEOLOGIC DESCRIPTIONS

To further investigate the relationship between the geologic descriptions and the computed V_{S30} P-wave seismogram estimates from this study, the 251 sites were grouped by attributes such as geologic age and rock type. Digital state-wide geologic maps compiled by the United States Geological Survey (USGS) Division of Mineral Resources (<http://mrddata.usgs.gov/geology/state/>) for Oklahoma and Kansas, as well as 1:250,000-scale geologic maps of Texas published by the Bureau of Economic Geology (BEG) at the University of Texas (Geologic Atlas of Texas series of 38 maps covering the entire state, <https://www.twdb.texas.gov/groundwater/aquifer/GAT/>), were used to assign these attributes. The geologic age groupings defined by Parker et al. (2017) were used. For each group, mean V_{S30} values (computed as the exponent of the natural log mean and designated $\mu_{\ln V}$) as well as natural log standard deviations ($\sigma_{\ln V}$) were computed.

Parker et al. (2017) defined 18 geologic age groups, and 7 of these groups are represented in the study area, as listed below:

- Group 1: Holocene alluvium
- Group 5: Pleistocene deposits that did not experience the Wisconsin glaciation
- Group 9: Undivided Quaternary deposits not in a sedimentary basin
- Group 12: Tertiary formations

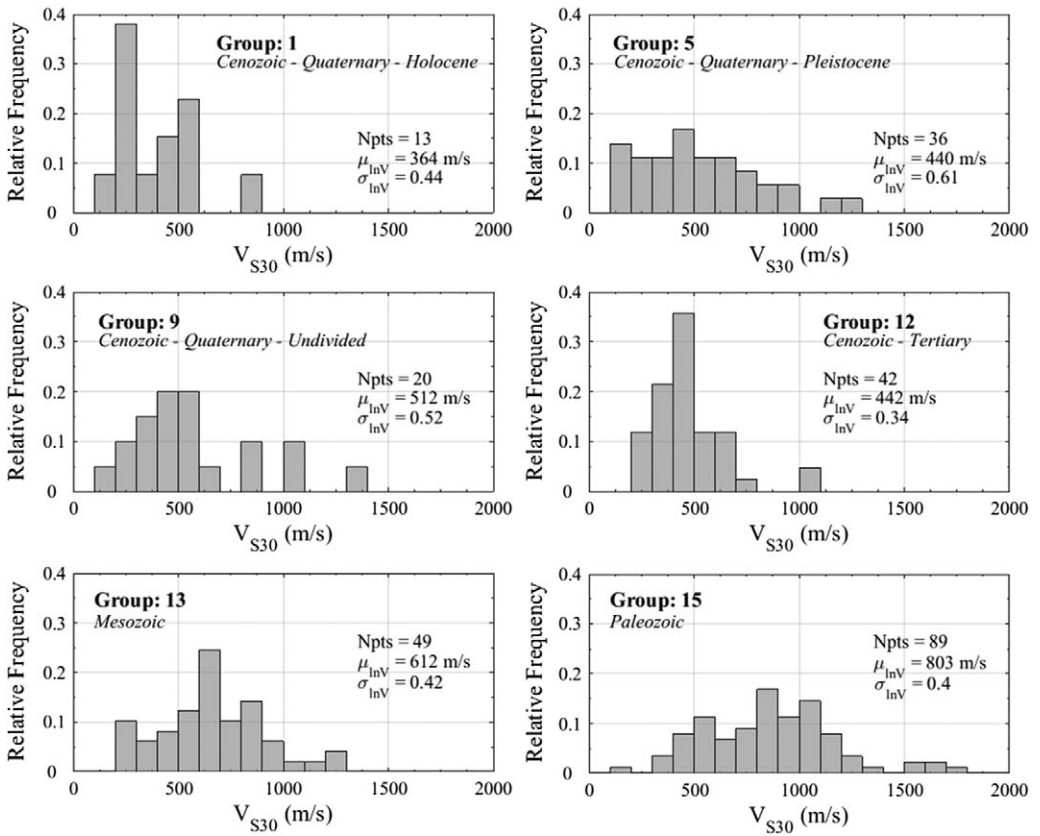


Figure 9. Histograms of P-wave seismogram V_{S30} estimates for different NGA-East geologic proxy groups.

- Group 13: Mesozoic formations
- Group 15: Paleozoic formations not in the Illinois Basin that did not experience the Wisconsin glaciation
- Group 17: Precambrian formations

In terms of rock type, the documented geologic descriptions were divided into six rock type groups based on the relative stiffness of the formations. Three groups represent different types of soil deposits and three groups represent soft-to-hard rock formations, as listed below:

- Group A: Alluvial and terrace deposits
- Group B: Clay, silt, and loess; not alluvium
- Group C: Sand and gravel; not alluvium
- Group D: Sedimentary formations of varying degrees of cementation; mudstone, claystone, siltstone, sandstone, conglomerate, marl, and shale
- Group E: Limestone, chalk, and evaporite
- Group F: Chert, basalt, granite, and rhyolite

Table 2. Mean V_{330} (μ_{inV}) and standard deviation (σ_{inV}) values for different geologic age and rock type groupings

NGA-East Group	Geologic Age	Rock Type Group	Parker et al. (2017)					
			Npts	μ_{inV} (m/s)	σ_{inV}	Npts	μ_{inV} (m/s)	σ_{inV}
1	Cenozoic - Quaternary - Holocene Alluvium	A/C	13	363	0.44	308	210	0.23
5	Cenozoic - Quaternary - Pleistocene	A/B/C	36	440	0.61	284	271*	0.36
9	Cenozoic - Quaternary - Undivided	A/B/C	20	512	0.52	154	296*	0.43
12	Cenozoic-Tertiary							
	All	B/C/D/F	42	442	0.34	111	315*	0.31
	Clay	B	13	349	0.25			
	Sand, gravel, sandstone, mudstone	C/D	28	478	0.30			
	Basalt	F	1	1077	N/A			
13	Mesozoic							
	All	C/D/E	49	612	0.42	20	822	0.68
	Sand/sandstone, clay/claystone, shale, marl	C/D	29	543	0.41			
	Limestone, chalk, evaporite	E	20	727	0.37			
15	Paleozoic							
	All	D/E/F	91	813	0.40	96	684	0.61
	Sandstone, mudstone, siltstone	D	74	756	0.39			
	Limestone, chalk, evaporite	E	12	981	0.27			
	Granite, chert	F	3	1578	0.05			
17	Precambrian							
	All	F	2	1434	0.01	37	699	0.85
15/17	Paleozoic/ Precambrian							
	Granite, chert, rhyolite	F	5	1519	0.06			

* Note: Parker et al. (2016) includes slope gradient term.

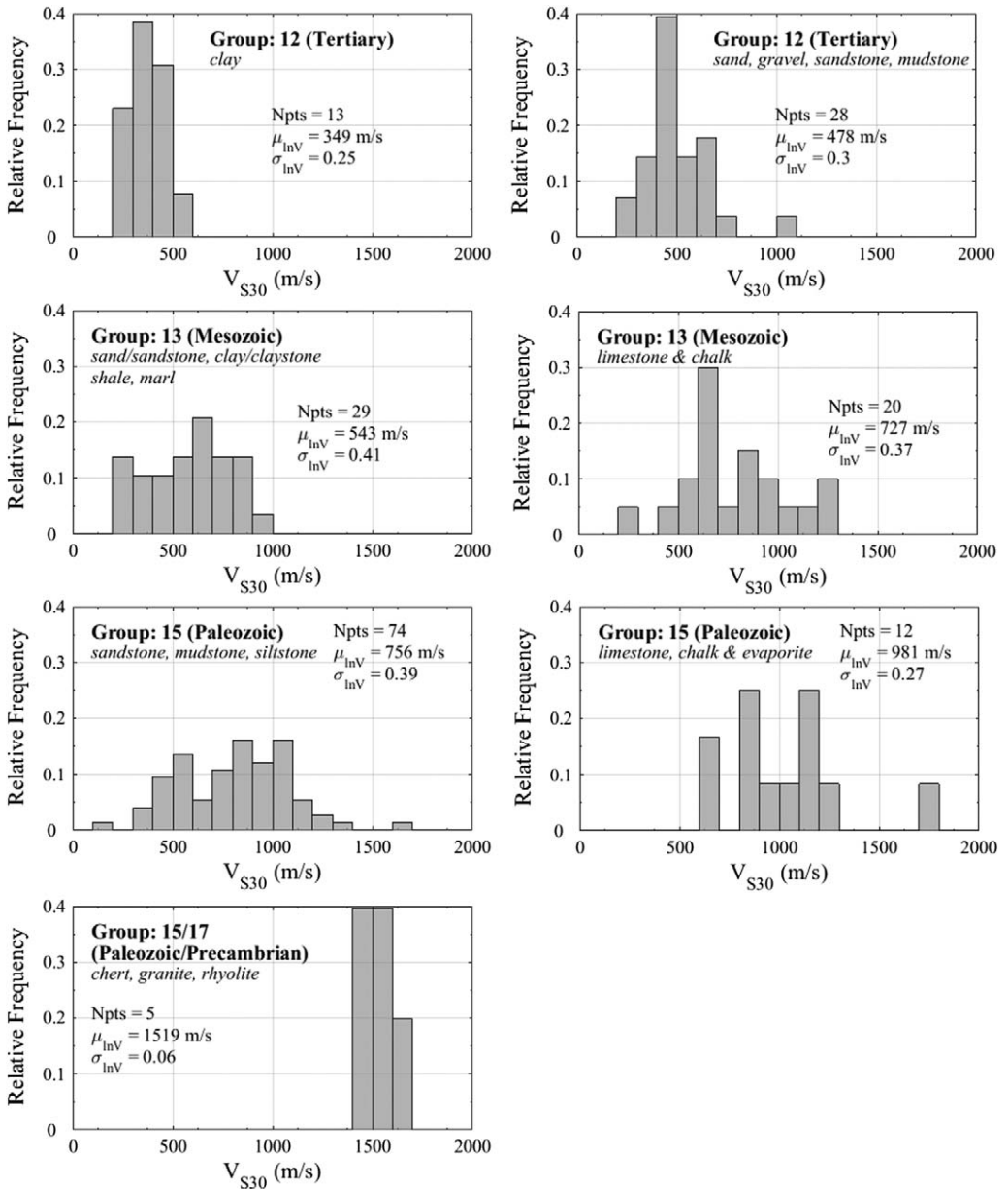


Figure 10. Histograms of P-wave seismogram V_{S30} estimates for revised NGA-East geologic proxy groups that distinguish rock type.

Figure 9 shows the histogram of the P-wave seismogram V_{S30} values for six of the geologic age groups from NGA-East. Group 17 (Precambrian) is not plotted because only two estimates are available for this group. The computed μ_{inV} and σ_{inV} are shown and these values are compared with those from Parker et al. (2017) in Table 2.

For the three Quaternary groups (Groups 1, 5, and 9), the $\mu_{\ln V}$ and $\sigma_{\ln V}$ from this study are larger than reported in Parker et al. (2017). The $\mu_{\ln V}$ are between about 360 m/s and 510 m/s for this study, while they are between 210 m/s and 300 m/s in Parker et al. (2017), and the $\sigma_{\ln V}$ are between about 0.45 and 0.6 for this study and between 0.23 and 0.43 in Parker et al. (2017). The differences are likely due to the fact that many of the Quaternary sites in the study area represent relatively narrow alluvial channels or wind-blown deposits with sediments that are relatively thin (i.e., less than 30 m). Many of the Quaternary sites included in the Parker et al. (2017) data set are from the broad alluvial basins, such as the Mississippi Embayment, which have deeper unconsolidated soil deposits and thus smaller V_{S30} . The five Quaternary sites from this study that are associated with thicker sediments along the Gulf Coast have $\mu_{\ln V}$ equal to 271 m/s, which is more consistent with the values reported by Parker et al. (2017).

For the Tertiary group (Group 12, Figure 9 and Table 2) the $\mu_{\ln V}$ is larger for this study (442 m/s vs. 315 m/s) but the $\sigma_{\ln V}$ are similar. For the Mesozoic group (Group 13), the $\mu_{\ln V}$ and $\sigma_{\ln V}$ are smaller for this study. And for the Paleozoic (Group 15) and Precambrian (Group 17) groups, the $\mu_{\ln V}$ are larger for this study but the $\sigma_{\ln V}$ are smaller. These differences are not surprising given that the study area for Parker et al. (2017) included the entirety of central and eastern North America, and this study is focused on a smaller study area. Indeed, only 78 of the 2,754 V_{S30} values in the Parker et al. (2017) data set were located in Texas, Oklahoma, or Kansas.

Our initial investigation of the histograms of sites separated based on rock type groups did not yield better results than those shown in Figure 9 for geologic age groups. However, separating the rock type groups within the older geologic age groups (Groups 12, 13, and 15) did result in a statistically significant improvement. Statistical differences were determined using the two F-tests described in Parker et al. (2017). The histograms for the separate rock type groups within these geologic age groups are shown in Figure 10 and the $\mu_{\ln V}$ and $\sigma_{\ln V}$ are listed in Table 2. For Tertiary Group 12, rock type group B (clay sites) display smaller $\mu_{\ln V}$ and $\sigma_{\ln V}$ than rock types C/D (sand/gravel/sandstone/mudstone/shale sites). For Mesozoic Group 13, rock types C/D display a significantly smaller $\mu_{\ln V}$ than rock type E (limestone/chalk, evaporite). For Paleozoic Group 15, rock type D displays a smaller $\mu_{\ln V}$ than rock type E which in turn has a smaller $\mu_{\ln V}$ than rock type F (granite, chert, rhyolite). In fact, the Paleozoic and Precambrian sites of rock type F are all very similar with $\mu_{\ln V}$ equal to 1,519 m/s and $\sigma_{\ln V}$ equal to 0.06.

DISCUSSION AND CONCLUSIONS

Estimates of V_{S30} at 251 seismic stations located within Texas, Oklahoma, and Kansas were developed using the P-wave seismogram method and a total of 2,871 earthquake recordings. Based on the P-wave seismogram V_{S30} values and inverse distance weighting, a preliminary V_{S30} map of the study area was created. This map captures the broad variations of V_{S30} across the study area, including regions of rock with V_{S30} greater than 1,000 m/s and unconsolidated sediments with V_{S30} less than 400 m/s.

For the limited locations where V_{S30} values derived from in-situ shear wave velocity measurements were available, the P-wave seismogram estimates of V_{S30} agreed favorably. Although, on average, the P-wave seismogram values were about 20% smaller than those

from in-situ measurements, this can be considered within the uncertainty of the measurements. This favorable comparison demonstrates that if in-situ measurements of shear wave velocity are not available, the P-wave seismogram approach can provide a high-quality estimate of V_{S30} for a seismic station.

Compared with the V_{S30} values assigned to the stations by the NGA-East hybrid slope-geology proxy technique (Parker et al. 2017), the P-wave seismogram method generally estimated larger V_{S30} values. Almost 50% of the sites analyzed in this study have P-wave seismogram V_{S30} values more than 25% larger than the NGA-East assigned values. These differences are likely due to differences in the characteristics of the geologic units in the study area relative to the characteristics of the sites in the V_{S30} database of Parker et al. (2017). Only 78 of the 2,754 in situ V_S measurements in Parker et al. (2017) were located in the study area of Texas, Oklahoma, and Kansas.

The geologic conditions (i.e., geologic age and rock type) at each P-wave seismogram V_{S30} site were documented using large scale geologic maps. For the geologic age groups used by Parker et al. (2017), the $\mu_{\ln V}$ and $\sigma_{\ln V}$ from this study were different than reported in Parker et al. (2017). Again, this result is likely due to differences in the geologic characteristics in the study area relative to the sites in Parker et al. (2017). The V_{S30} values from the present study also indicate that it is important to differentiate between rock types within the Tertiary, Mesozoic, Paleozoic, and Precambrian geologic age groups. Statistical differences in terms of both $\mu_{\ln V}$ and $\sigma_{\ln V}$ were observed among the different rock types present in these geologic age groups (Table 2).

Based on this study, the following protocols are recommended for assigning V_{S30} values to seismic stations in Texas, Oklahoma, and Kansas. In-situ measurement of shear wave velocity is always preferred and should be used if at all possible. If in-situ measurements are not available, V_{S30} values derived using the P-wave seismogram method should be used because they are based on site-specific data. Finally, if neither in-situ V_S measurements nor P-wave seismogram V_{S30} estimates are available, then proxy techniques should be employed. For sites in Texas, Oklahoma, and Kansas, the combined geologic age and rock type proxy groups shown in Figures 9 and 10, and Table 2, should be used to assign V_{S30} to sites rather than the NGA-East hybrid slope-geology proxy technique (Parker et al. 2017) because few in-situ V_S measurements in Texas, Oklahoma, and Kansas were used in the development of the NGA-East proxy method.

Finally, although the P-wave seismogram V_{S30} values derived in this study were consistent with the general geologic conditions across the study area and agreed well with limited in-situ V_S measurements, additional site-specific validation of its performance and variability is needed. In situ V_S profile measurements at different seismic stations and within different geologic units of Texas, Oklahoma, and Kansas are required for this validation. A regional V_{SZ} to V_{S30} conversion would also improve the V_{S30} estimates from the P-wave seismogram method.

ACKNOWLEDGMENTS

This work was sponsored through funding from the State of Texas through the TexNet Seismic Monitoring Project, from the Industrial Associates of the Center for Integrated Seismic Research (CISR) at the Bureau of Economic Geology of the University of Texas, and

from the Texas Department of Transportation under Project 0-6916. This funding is gratefully acknowledged. This work also benefited significantly from interactions with the NGA-East Geotechnical Working Group, in particular Grace Parker, Byungmin Kim, Jonathan Stewart, and Youssef Hashash.

REFERENCES

- Abrahamson, N. A., Silva, W. J., and Kamai, R., 2014. Summary of the Abrahamson, Silva, and Kamai NGA-West 2 ground-motion relations for active crustal regions, *Earthquake Spectra* **30**, 1025–1055.
- Aki, K., and Richards, P. G., 2002. *Quantitative Seismology*, University Science Books, Sausalito, CA, 700 pp.
- Boore, D. M., Stewart, J. P., Seyhan, E., and Atkinson, G. M., 2014. NGA-West2 Equations for Predicting PGA, PGV, and 5% Damped PSA for Shallow Crustal Earthquakes, *Earthquake Spectra* **30**, 1057–1085.
- Dreiling, J., Isken, M. P., Mooney, W. D., Chapman, M. C., and Godbee, R. W., 2014. NGA-East Regionalization Report: Comparison of Four Crustal Regions within Central, and Eastern North America using Waveform Modeling, and 5%-Damped Pseudo-Spectral Acceleration Response, *PEER Report 2014/15*. PEER, Berkeley, CA, available online at: http://peer.berkeley.edu/publications/peer_reports.html.
- Electric Power Research Institute (EPRI), 1993. Guidelines for determining design basis ground motions, *Report No. TR-102293*, Palo Alto, CA.
- Goulet, C. A., Kishida, T., Ancheta, T. D., Cramer, C. H., Darragh, R. B., Silva, W. J., Hashash, Y. M. A., Harmon, J.A., Stewart, J. P., Wooddell, K. E., and Youngs, R. R., 2014. PEER NGA-East Database, *PEER Report 2014/17*, Pacific Earthquake Engineering Research Center, Berkeley, CA. Available online at: http://peer.berkeley.edu/publications/peer_reports.html.
- Hosseini, M., Somerville, P., Skarlatoudis, A., Bayless, J., and Thio, H. K., 2016. Constraining shallow subsurface S wave velocities with the initial portion of local P waves recorded at multiple seismic networks including ANSS, and EarthScope Transportable Array in the CEUS, *Final Technical Report Award Number: G14AP00110*.
- Incorporated Research Institutions for Seismology (IRIS), available at <https://www.iris.edu/hq/>.
- Kim, B., Hashash, Y. M. A., Rathje, E. M., Stewart, J. P., Ni, S., Somerville, P. G., Kottke, A. R., Silva, W. J., and Campbell, K. W., 2016. Subsurface shear-wave velocity characterization using P-wave seismograms in central, and eastern North America, *Earthquake Spectra* **32**, 143–169.
- Kottke, A. R., Hashash, Y. M. A., Stewart, J. P., Moss, C. J., Nikolaou, S., Rathje, E. M., Silva, W. J., and Campbell, K. W., 2012. Development of geologic site classes for seismic site amplification for central, and eastern North America, Paper No. 4557, in *Proc. 15th World Conf. on Earthquake Eng.*, 24–28 September 2012, Lisbon, Portugal.
- Ni, S, Li, Z., and Somerville, P., 2014. Estimating subsurface shear velocity with radial to vertical ratio of local P-waves, *Seismol. Res. Lett.* **85**, doi: 10.1785/0220130128.
- Pacific Earthquake Engineering Research Center (PEER), 2015. *NGA-East: Median Ground-Motion Models for Central and Eastern North America*, PEER Report 2015/04, PEER, Berkeley, CA, available at http://peer.berkeley.edu/publications/peer_reports.html.
- Parker, G. A., Harmon, J. A., Stewart, J. P., Hashash, Y. M. A., Kottke, A. R., Rathje, E. M., Silva, W., and Campbell, K. W., 2017. Proxy-based V_{S30} estimation in central, and eastern North America, *Bull. Seis. Soc. Am.*, accepted for publication.

- Petersen, M. D., Moschetti, M. P., Powers, P. M., Moschetti, M. P., Hoover, S. M., Llenos, A. L., Ellsworth, W. L., Michael, A. J., Rubinstein, J. L., McGarr, A. F., and Rukstales, K. S., 2016. *One-Year Seismic Hazard Forecast for the Central and Eastern United States from Induced and Natural Earthquakes*, U.S. Geological Survey Open-File Report 2016–1035, 58 pp.
- United States Geological Survey (USGS) Division of Mineral Resources (DMR). *State-Wide Geologic Maps*, available at <https://mrdata.usgs.gov/geology/state/>.
- Wald, D. J., and Allen, T. I., 2007. Topographic slope as a proxy for seismic site conditions, and amplification, *Bull. Seis. Soc. Am.* **97**, 1379–1395.
- Wills, C. J., and Clahan, K. B., 2006. Developing a Map of Geologically Defined Site-Condition Categories for California, *Bull. Seis. Soc. Am.* **96**, 1483–1501.
- Yong, A., Hough, S. E., Iwahashi, J., and Braverman, A., 2012. A terrain based site conditions map of California with implications for the contiguous United States, *Bull. Seismol. Soc. Am.*, **102**, 114–12.
- Zalachoris, G., Rathje, E., Cox, B., and Chen, T., 2017. Application of the P-wave seismogram method for V_{S30} characterization of Texas, Oklahoma, and Kansas, *3rd International Conference on Performance-Based Design in Earthquake Geotechnical Engineering*, Vancouver, BC, Canada.

(Received 24 October 2016; accepted 15 February 2017)